

Observation of anomalous conical emission from laser-excited barium vapor

C. H. Skinner and P. D. Kleiber*

Joint Institute for Laboratory Astrophysics, University of Colorado and National Bureau of Standards, Boulder, Colorado 80309

(Received 30 July 1979)

The authors have observed an anomalous emission feature from a dense ($\sim 10^{16}$ cm $^{-3}$) barium vapor illuminated with a N $_2$ pumped dye laser (peak intensity ~ 1 MWcm $^{-2}$). The input laser wavelength was 552.5 nm, 1 nm shorter in wavelength than the barium $6s^2^1S-6s6p^1P$ resonance transition. In the forward direction strong emission was observed emerging from the barium vapor in the form of an conical shell of half-angle $\sim 2^\circ$ at $\sim 1\%$ of the incident laser intensity. The emission was broad in wavelength (3 nm) and peaked 1 nm longer in wavelength than the Ba $6s^2^1S-6s6p^1P$ transition. Self-focusing of the laser beam by the barium vapor was observed under the same conditions. Although the emission is intense, an adequate explanation of this phenomenon has yet to be found.

I. INTRODUCTION

Conical anti-Stokes emission was observed in the early days of stimulated electronic Raman scattering in liquids, and the cone angle related to phase-matching requirements.¹ The interpretation of some of the experimental data was complicated by the occurrence of self-focusing of the input laser beam.^{2,3} More recently in studies of self-focusing in atomic vapors there have been reports^{4,5} of anomalous off-axis emission which are apparently unrelated to Raman scattering and for which no adequate explanation has been offered.

We have observed conical emission when high-density ($\sim 10^{16}$ cm $^{-3}$) barium vapor was illuminated by a N $_2$ pumped dye laser, tuned 1 nm on the short-wavelength side of the $6s^2^1S-6s6p^1P$ barium resonance transition. The emission was surprisingly intense. In an effort to understand this phenomenon, we undertook a systematic study of the cone emission angle, spectrum, polarization, and intensity as a function of laser polarization, wavelength, intensity, and barium density, and the results are described below.

II. EXPERIMENTAL ARRANGEMENT

The experimental arrangement is shown in Fig. 1. A pulsed 1-MW N $_2$ laser was used to pump transversely a dye laser in the standard arrangement⁶ with a 10 \times beam expander and an Echelle grating (316 lines/mm). The dye-laser beam was linearly polarized, 0.02 nm in bandwidth with peak intensity of 1 MW cm $^{-2}$ and duration 7 nsec. The laser was operated in the spectral region near 553.5 nm, the wavelength of the barium $6s^2^1S-6s6p^1P$ resonance transition. The unfocused laser beam was directed through a stainless steel heat-pipe oven.⁷ The heat-pipe oven was constructed in the form of a cross and lined with nickel mesh. The entrance and exit windows

were tilted at an angle of 30° to the laser axis to prevent multiple reflections. The heat-pipe was loaded with ~ 50 g of barium and the central region heated to 1070 $^\circ$ C. Argon was used to contain the barium vapor, the barium vapor pressure being equal to the argon pressure in the heat-pipe mode. Heat-pipe action was verified by the observation of 90° Rayleigh scattering of the laser beam by the barium, since a linear relation between scattered flux and argon pressure was observed in the region 0.1–0.8 torr. In order to control the buildup of solid barium at the cool ends of the furnace tubes, the furnace was equipped with independently controlled heater coils for the outer 3 cm of the heated region and movable water cooling jackets. By temporarily raising the temperature of the outer sections from 900 to 1050 $^\circ$ C and moving the cooling jackets back ~ 1 cm, any solid barium deposits could be quickly remelted. The column length of barium was determined by measurements of the Ba 553.5-nm absorption profile. The observed absorption was compared to the calculated absorption coefficient due to resonance broadening, the value of the C_3 constant being derived from the literature oscillator strength.⁸ The result of 8 cm was consistent with the furnace geometry, and is a further check on functioning of the heat-pipe. An internal 2-mm-diam aperture was placed inside the oven to provide a well-defined laser-illuminated region.

III. EXPERIMENTAL STUDIES

A. Cone angle

Observation of the light emerging from the oven in the forward direction when the laser wavelength was set at 552.5 nm revealed an intense conical shell of light surrounding the central laser spot. In addition, the laser spot itself was more diffuse than in the absence of barium. The cone was recorded photographically by a Polaroid film back

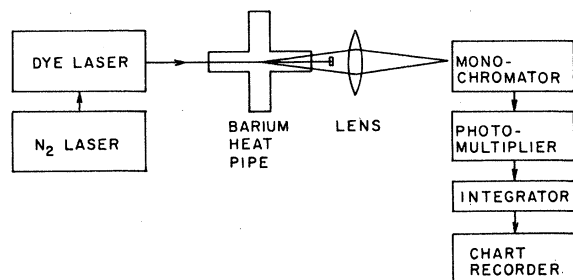


FIG. 1. Basic experimental arrangement.

placed after the oven (without any imaging optics) (see Fig. 2.) The cone angle was calculated from geometry. Figures 3 and 4 show the variation in cone angle with barium density and laser detuning. In comparison, Tam⁵ reported a similar variation of cone angle with density but did not observe any dependence of cone angle on laser detuning. The cone angle was found to be independent of input laser intensity.

B. Cone spectrum

The cone spectrum was measured by imaging the center of the oven onto the entrance slit of a 0.6-m monochromator equipped with a 2400-lines/mm holographic grating and an RCA 7326 photomultiplier. The signal was detected with a gated integrator, averaged over ~ 20 laser shots, and displayed on a chart recorder. The direct laser light was blocked by a 12-mm-diam disc placed on axis. Calibrated neutral-density filters (attenuation $\sim 10^5$) were used to avoid saturating the detector. The spectrum is shown in Fig. 5. There is some residual scattered light at laser wavelength with, however, a significantly higher bandwidth (0.2 nm) than the incident laser (0.02 nm) (see Sec. III F). There is also a broad (3-nm) feature which peaks at 554.5 nm. This peak and the laser wavelength were symmetrically located at approximately equal detunings from the Ba 553.5-

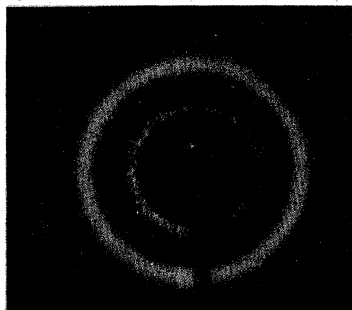
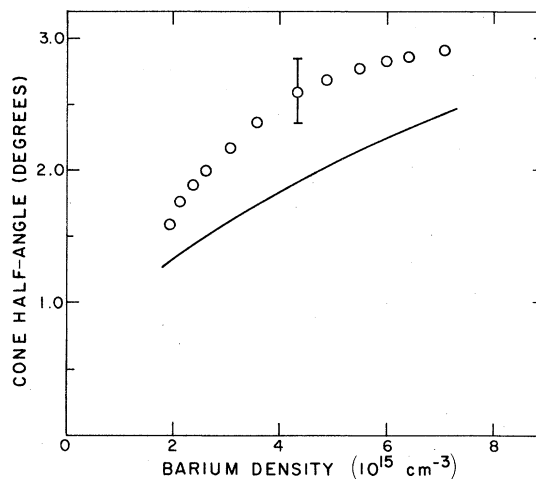
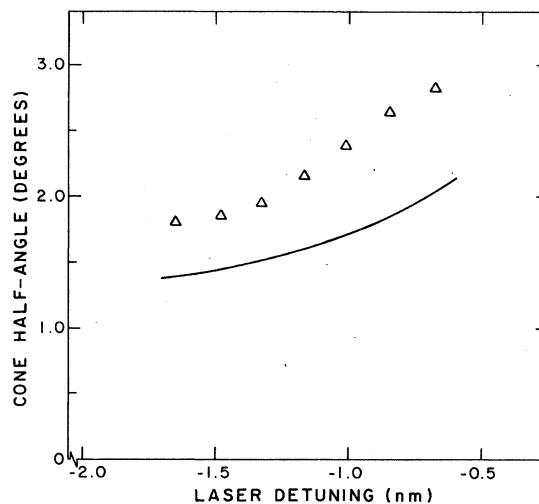


FIG. 2. Photograph of conical emission. For clarity, the laser beam was blocked with a small disc placed on axis.

FIG. 3. Cone angle vs barium density. The laser detuning was -1.0 nm. The solid line is a theoretical curve based on a hypothetical parametric mixing scheme. The vertical line represents the angular spread of the cone.

nm transition (λ_0). This is in contrast to the result of Tam,⁵ who reports a broad spectral feature apparently on the *short*-wavelength side of the resonance line. However, in his case the absolute wavelength calibration is uncertain owing to the multiple orders of the analyzing Fabry-Perot.⁹ Spatial scans at 554.5 nm identified the broad feature with the observed cone. A spectral scan at high (8-pm) resolution showed the cone spectrum to be smooth on that wavelength scale. The angular spread of the cone emission was $\sim 0.5^\circ$ and the spectrum of Fig. 5 includes the complete angular

FIG. 4. Cone angle vs laser detuning. Barium density was $3.6 \times 10^{15} \text{ cm}^{-3}$. The solid line is a theoretical curve based on a hypothetical parametric mixing scheme.

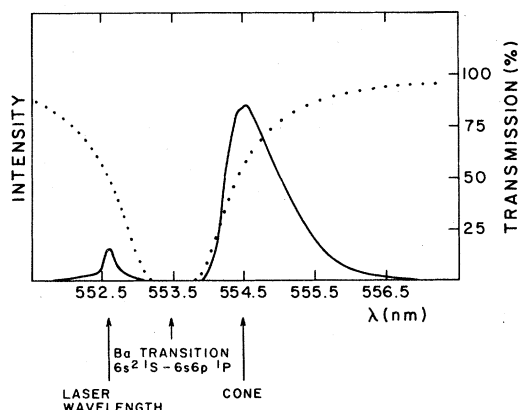


FIG. 5. Cone spectrum (solid line). The barium density was $5.2 \times 10^{15} \text{ cm}^{-3}$ and input laser intensity was 0.64 MW cm^{-2} . Note the small feature at the laser wavelength. This feature is not emitted in a cone and is $10 \times$ broader in wavelength than the incident laser. The low-intensity transmission is also plotted (dotted line). This represents the transmission from the oven center to the outside under the conditions in which the cone spectrum was measured (see text).

range. Angle and wavelength resolutions were achieved in a different arrangement, whereby a radial section of the cone was directed to the monochromator entrance slit and the spectrum recorded photographically. The results indicated that the cone spectrum was broad at all angles; there was, however, a small shift of $\sim +0.4 \text{ nm}$ of the short-wavelength edge of the cone spectrum with increasing angle from the laser axis. In order to determine whether the cone spectrum was influenced by absorption by the Ba 553.5-nm transition, the transmission spectrum of a tungsten lamp through the heat-pipe oven was measured. Figure 5 shows the transmission at a barium density 56% of that at which the cone spectrum was measured and thus represents the transmission from close to the oven center to the outside at the density at which the cone was measured. It can be seen that the cone is generated in a spectral region of significant absorption.

C. Conversion efficiency

The conversion efficiency of laser-to-cone radiation was measured by comparing the spectrum of the laser (with no barium present and the 12-mm laser block removed) to that of the cone measured with the same optical arrangement (but with barium and block in place). For an incident laser intensity of 0.5 MW cm^{-2} , detuning 1.0 nm, and barium density $6 \times 10^{15} \text{ cm}^{-3}$, the ratio of the intensity, integrated over wavelength, of the cone to the incident laser was $1\%_{-0.5\%}^{+1\%}$, a remarkably high fig-

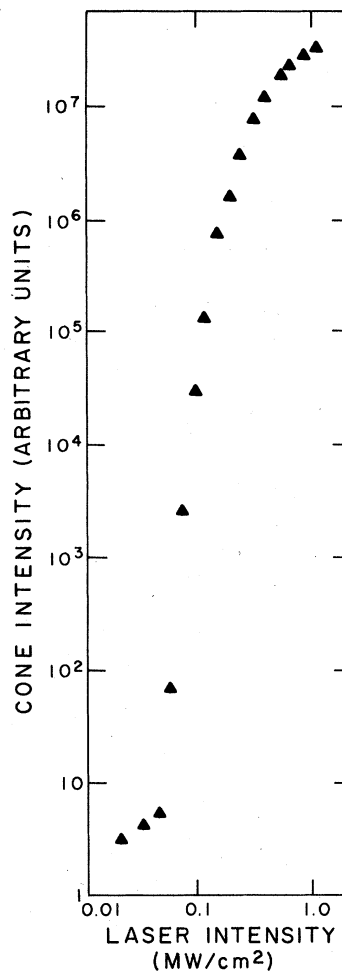


FIG. 6. Cone intensity vs input laser intensity. The barium density was $4.9 \times 10^{15} \text{ cm}^{-3}$. The linear region at very low intensity is due to scattered laser light. Note the very rapid turn-on at input laser intensities above 0.1 MW cm^{-2} .

ure. In comparison, Mahon¹⁰ obtained a 10^{-5} conversion for frequency tripling in xenon with a 6-MW laser.

D. Cone polarization

The cone radiation was linearly polarized ($>99\%$) in the same direction as the incident laser. An experiment in which a Fresnel rhomb was used to convert the laser from linear to circular polarization yielded cone radiation that was circularly polarized in the same sense as the laser.

E. Cone spectrum versus laser intensity, laser wavelength, and barium density

The cone was further studied as a function of three experimental parameters: laser intensity,

laser wavelength, and barium density. In the first experiment the laser was attenuated with calibrated neutral-density filters. The peak cone intensity was strongly dependent on laser intensity, as can be seen in Fig. 6. However, the cone spectrum was insensitive to changes in laser intensity. For a factor-of-10 decrease in input laser intensity the spectral width of the cone was reduced by only 5% and the peak wavelength was unchanged. The cone spectrum was observed to vary with laser wavelength (Fig. 7). The cone peak wavelength was always close to the opposite detuning to the laser (Fig. 8), and the cone spectral width increased in proportion to the detuning. For laser detunings $\lambda_L - \lambda_0$ in the region from -1.3 to -0.7 nm the cone intensity was constant within a factor of 3. Outside that region it decreased, no cone being observed for detunings < -1.8 or > -0.4 nm.

The barium density was varied by changing the argon pressure and the cone spectrum measured over a range of barium densities $2-6 \times 10^{15} \text{ cm}^{-3}$. At maximum laser intensity ($\sim 1 \text{ MW cm}^{-2}$) the peak cone intensity was independent of barium density. The cone spectrum did extend closer to the Ba 553-nm line at low densities showing the effect of reduced absorption. A feature on the short-wavelength side of the cone spectrum similar to that shown in Fig. 7 (solid curve, at 554 nm), but at 553.9 nm, was present at the lowest densities. No corresponding feature was present in the barium absorption spectrum. The same experiment performed at reduced laser intensities (0.1 MW cm^{-2}) showed a strong dependence (approximately N^3) of cone intensity on barium density.

F. Laser broadening

In addition to the generation of the cone, the laser spectrum was "broadened" by transmission

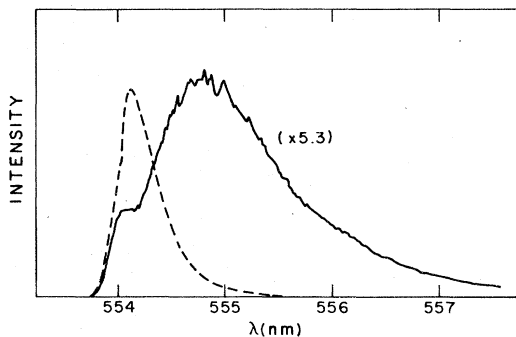


FIG. 7. Cone spectrum vs laser detuning. The solid (dotted) line corresponds to a laser detuning of -1.43 nm (-0.47 nm). The barium density was $3.6 \times 10^{15} \text{ cm}^{-3}$ and the input laser intensity 0.7 MW cm^{-2} . The intensity of the solid curve has been multiplied by 5.3.

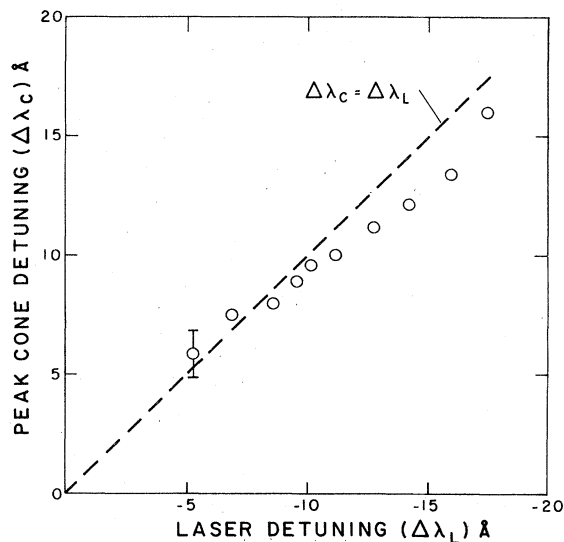


FIG. 8. Wavelength of the peak of the cone spectrum vs laser wavelength. A typical error bar is shown. The barium density was $3.6 \times 10^{15} \text{ cm}^{-3}$.

through the barium vapor. This can be seen in Fig. 5, where light scattered at small angles was detected, the central laser spot being blocked. A high-resolution scan of the complete laser spectrum without the central block is shown in Fig. 9, and it can be seen that there is substantial additional emission outside the input laser spectrum. This could be detected up to 1 nm from the central laser wavelength. A possible explanation is discussed in Sec. IV.

The spectrum of forward-scattered light with

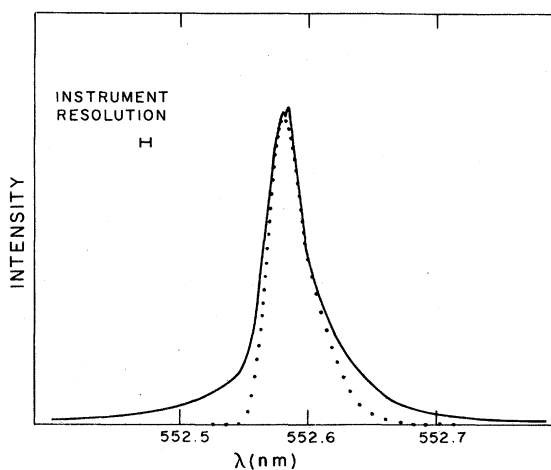


FIG. 9. Normalized laser spectrum (dotted line) as modified by barium (solid line). The barium density was 5.2×10^{15} , input laser intensity 0.7 MW cm^{-2} . The instrumental resolution was 8 pm; the absolute wavelength calibration of each curve was accurate to 0.05 nm.

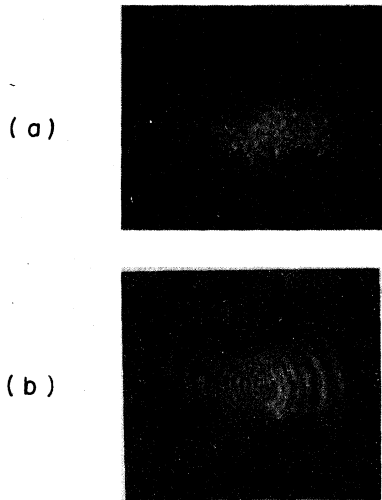


FIG. 10. Photograph of laser beam at oven center with (a) input laser intensity 0.2 MW cm^{-2} , (b) input laser intensity 0.02 MW cm^{-2} .

the laser wavelength set to 554.5 nm (on the long-wavelength side of the barium transition) was also measured. Broad emission was observed in the region 554–556 nm at an intensity (integrated over wavelength) and 10^{-3} – 10^{-5} of the laser. The spectral intensity was strongly dependent on laser intensity. Direct observation of the laser beam after the oven revealed a defocused laser spot but no cone.

G. Self-focusing

A key observation in the experiment was the detection of self-focusing of the laser beam by the barium vapor. In this part of the experiment the center of the oven was imaged, using two camera lenses, onto a Polaroid film back at high ($\times 20$) magnification. Photographs were obtained of the laser beam inside the oven under the same sets of experimental conditions described in Sec. III A–III F. Typical results are shown in Fig. 10. The image obtained at low intensity shows a smooth intensity distribution modulated by diffraction arising from the 2 mm aperture. (Removal of this aperture did not affect the generation of the cone radiation or self-focusing.) However, at input laser intensities $>0.1 \text{ MW cm}^{-2}$ the image was observed to break up into hundreds of individual foci. This occurred over exactly the same range of laser intensity, wavelength, and barium density that led to the generation of the cone. Outside this range no foci were present.

IV. DISCUSSION

The most salient feature of the cone emission is its spatial character, suggestive of phase matching

in a parametric frequency-mixing process. We calculate the cone angle for a hypothetical four-wave mixing process in which the laser at frequency ω_L combines with two other waves ω_1 and ω_2 assumed collinear with the laser to generate a new frequency ω_c at an angle θ . The refractive index in the vicinity of the barium transition, ω_0 , is given by the classical formula

$$n(\omega) = 1 + \pi e^2 f(N_1 - N_2) / m\omega_0(\omega_0 - \omega). \quad (1)$$

Here e and m are the electronic charge and mass, f is the atomic oscillator strength, and N_1 and N_2 are the $6s^2^1S$ and $6s6p^1P$ barium densities. For simplicity, we take the case of $N_1 \gg N_2$ (unrealistic in a self-focused filament). Complete phase matching in three dimensions is not possible, so we use the surface phase-matching relation² and equate the axial components of the wave vectors k ($k = n\omega/c$) of the four waves:

$$n(\omega_c)\omega_c \cos\theta = n(\omega_L)\omega_L \pm n(\omega_1)\omega_1 \pm n(\omega_2)\omega_2.$$

We take the case in which ω_1 and ω_2 are in a frequency region where the refractive index is unity. The value of $\omega_1 \pm \omega_2$ is determined by energy conservation; ω_L and ω_c are known from experiment. The results are shown in Figs. 3 and 4.

It can be seen that the relationship is close in absolute value and has the same functional form as the experimental data. However, a fundamental difficulty arises when an experimental search is made for the additional waves ω_1 and ω_2 , or possible theoretical mechanisms for their generation are considered. In order to obtain the high conversion efficiency observed experimentally, the additional waves ω_1 and ω_2 must be comparable in intensity to the laser and hence easy to detect. Three methods were tried. First, we made a complete visible-wavelength scan from 240 to 850 nm, using the monochromator to detect any forward emission with an intensity greater than 10^{-4} of that of the laser. Second, a calorimeter was placed on axis after the oven. Here the wavelength range detectable was 0.6–2.7 μm and sensitivity was $\sim 5\%$ of the laser intensity. Third, a second dye laser was constructed in an attempt to up-convert infrared radiation in the 70–500 μm region via a two-photon transition which would decay by visible fluorescence. This scheme was calibrated by measuring 90° Rayleigh scattering; in theory, infrared radiation at the same intensity as that of the cone would be detectable. All of these methods gave a null result, indicating that a conventional parametric mixing is unlikely to be able to account for the cone generation.

An alternative explanation may be sought in the results of Tam,⁵ who reports amplification of laser sidebands in a Raman-type process. We also

observe a considerable increase in intensity in the laser spectral wings after transmission through the barium vapor. However, a similar Raman process is ruled out, since the barium ground state ($6s^2\ ^1S_0$) is a single level. To check experimentally if the cone was due to amplification of possible far-laser wings, we repeated our experiment, but with the laser prefiltered by a monochromator with a 0.5-nm bandpass. The cone radiation was still observed, indicating the cone was not generated by amplification of laser sidebands.

Stimulated transitions in excited molecular barium were considered, e.g.,



The parentheses contain the separated atomic states. Here the spectral width of the cone may be interpreted as being due to level shifts of the molecular states with internuclear separation. However, a major difficulty is understanding how such emission could be generated in a cone.

Self-focusing^{11,12} in atomic vapors occurs through the N_1 - N_2 factor in Eq. (1). On the high-frequency side of the transition the refractive index increases with laser intensity owing to population of level 2 by the laser. In an inhomogeneous laser beam a positive lens effect results and the beam self-focuses to the point where $N_2 \approx N_1$ and the further contraction of the beam is offset by diffraction. On the low-frequency side, light is defocused. In the present experiment the observation of the cone was exactly correlated with the observation of self-focusing. Self-focusing obviously increases the laser intensity and can enhance any nonlinearities. Frequency broadening on the scale of several nan-

ometers has been observed¹² in nanosecond laser pulse excitation of CS_2 . Here the rapid changes in refractive index due to the self-focused laser pulse give rise to phase modulation and hence frequency broadening. This effect may account for the increased spectral width of the laser after transmission through the barium vapor. In addition, the observed (see Sec. III E) inter-relationship between cone intensity, barium density, and laser intensity may be understood qualitatively in terms of the critical power¹² necessary for self-focusing. Shen¹² has developed a moving-focus model in which the locus of the focal spot moves at velocities exceeding the velocity of light. This may give rise to Čerenkov radiation¹³ which would be emitted in the form of a cone. The direction of polarization of the light is not expected to be changed by such a process, and this might account in a natural way for our observation that the cone has the same polarization as the input laser. However, a detailed comparison to the present experiment is difficult.

It is clear that no complete explanation of the cone emission may be offered at the present time. This is all the more surprising, since it is far from being a small effect. It is hoped that the present paper will stimulate some theoretical work on the subject.

ACKNOWLEDGMENTS

We wish to thank G. Pichler for a discussion which led to our observation of this phenomenon. We also acknowledge useful discussions with J. L. Carlsten and A. Szöke. This work was supported by NSF Grant No. PHY76-04761.

*Also at Dept. of Physics and Astrophysics, Univ. of Colorado, Boulder, Col. 80309.

¹A. Yariv, *Quantum Electronics* (Wiley, New York, 1967).

²E. Garmire, in *Physics of Quantum Electronics*, edited by P. L. Kelley, B. Lax, and P. E. Tannenwald (McGraw-Hill, New York, 1966), pp. 167-179.

³K. Shimoda, *Jpn. J. Appl. Phys.* **5**, 86 (1966).

⁴D. Grischkowsky, *Phys. Rev. Lett.* **24**, 866 (1970).

⁵A. Tam, *Phys. Rev. A* **19**, 1971 (1979).

⁶T. W. Hansch, *Appl. Opt.* **11**, 895 (1972).

⁷C. R. Vidal and J. Cooper, *J. Appl. Phys.* **40**, 3370 (1969).

⁸B. M. Miles and W. L. Weise, *At. Data* **1**, 1 (1969).

⁹A. Tam (private communication).

¹⁰R. Mahon, T. J. McIlrath, and D. W. Koopman, *Appl. Phys. Lett.* **33**, 305 (1978).

¹¹A. Javan and P. L. Kelley, *IEEE J. Quantum Electron.* **QE2**, 470 (1966).

¹²Y. R. Shen, *Prog. Quantum Electron.* **4**, 1 (1975).

¹³G. A. Askar'yan, *Sov. Phys. JETP* **15**, 943 (1962).

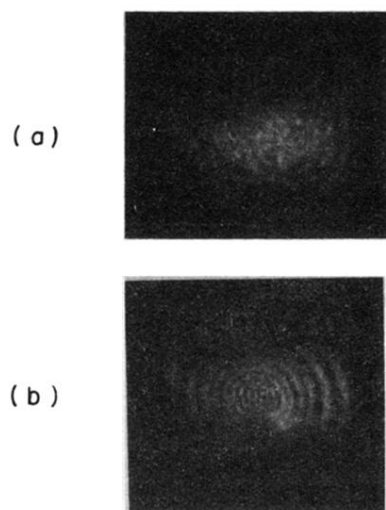


FIG. 10. Photograph of laser beam at oven center with (a) input laser intensity 0.2 MW cm^{-2} , (b) input laser intensity 0.02 MW cm^{-2} .

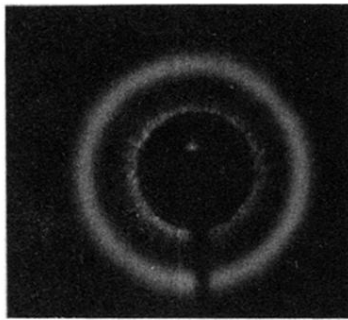


FIG. 2. Photograph of conical emission. For clarity, the laser beam was blocked with a small disc placed on axis.